Since January 2020 Elsevier has created a COVID-19 resource centre with free information in English and Mandarin on the novel coronavirus COVID-19. The COVID-19 resource centre is hosted on Elsevier Connect, the company's public news and information website.

Mathematical Biosciences 328 (2020) 108441

Contents lists available at ScienceDirect

Mathematical Biosciences

journal homepage: www.elsevier.com/locate/mbs

Original Research Article

Modeling the transmission dynamics of the COVID-19 Pandemic in South Africa

Salisu M. Garba [a], Jean M.-S. Lubuma [a,*], Berge Tsanou [a,b]

[a] Department of Mathematics and Applied Mathematics, University of Pretoria, Pretoria 0002, South Africa
[b] Department of Mathematics and Computer Sciences, University of Dschang, P.O. Box 96 Dschang, Cameroon

ARTICLE INFO

This paper is dedicated to the memory of Professor Anton Carel Stoltz (1 April, 1961 to 20 May, 2020), an outstanding epidemiologist, who passed away a few weeks after the launch of the University of Pretoria Biomath Response to COVID-19.

Keywords:
COVID-19
Control reproduction number
Isolation
Social-distancing
Environmental contamination

ABSTRACT

Since its emergence late in 2019, the COVID-19 pandemic continues to exude major public health and socio-economic burden globally. South Africa is currently the epicenter for the pandemic in Africa. This study is based on the use of a compartmental model to analyze the transmission dynamics of the disease in South Africa. A notable feature of the model is the incorporation of the role of environmental contamination by COVID-infected individuals. The model, which is fitted and parametrized using cumulative mortality data from South Africa, is used to assess the impact of various control and mitigation strategies. Rigorous analysis of the model reveals that its associated continuum of disease-free equilibria is globally-asymptotically stable whenever the control reproduction number is less than unity. The epidemiological implication of this result is that the disease will eventually die out, particularly if control measures are implemented early and for a sustainable period of time. For instance, numerical simulations suggest that if the lockdown measures in South Africa were implemented a week later than the 26 March, 2020 date it was implemented, this will result in the extension of the predicted peak time of the pandemic, and causing about 10% more cumulative deaths. In addition to illustrating the effectiveness of self-isolation in reducing the number of cases, our study emphasizes the importance of surveillance testing and contact tracing of the contacts and confirmed cases in curtailing the pandemic in South Africa.

1. Introduction

A novel Severe Acute Respiratory Syndrome Coronavirus 2 (SARS-CoV-2) was identified in December 2019 as the cause of an outbreak of a viral pneumonia in Wuhan (capital of Hubei, China) [1]. The disease, later named Coronavirus Identified in 2019 (COVID-19), quickly spread to more than 215 countries across all regions of the world [2], causing in excess of 14,5 million infections and more than 606,000 deaths globally, with South Africa recording about 364,324 cases (as of 20 July 2020) [1–3]. SARS-CoV-2, the causative agent of this highly contagious infectious disease, is closely related to the SARS virus [1]. There are many different types of coronaviruses, most of which are circulating among animals [4]. However, seven types of coronavirus are known to spillover from animals to humans, causing illnesses in humans. Three of the seven human coronaviruses can be much more severe (with mild to severe upper respiratory tract illness that causes symptoms of the common cold) and have recently caused major outbreaks of deadly pneumonia [4]. They are outlined as follows:

(1) SARS-CoV was first identified in China in 2002 as the cause of an outbreak of Severe Acute Respiratory Syndrome (SARS). It causes flu-like symptoms. In May 2004, the World Health Organization (WHO) [5] declared that SARS was contained (eradicated) worldwide.
(2) MERS-CoV was first identified in 2012 in Jordan and Saudi Arabia as the cause of Middle East Respiratory Syndrome (MERS). It causes flu-like symptoms. MERS-CoV has been circulating in several countries (*e.g.* USA, May 2014; South Korea, July 2015) and is still around (2200 confirmed cases and 790 deaths in 2018) [4].
(3) SARS-CoV-2 was identified in December 2019. It causes acute respiratory illness that can be severe.

Studies in the literature suggest that SARS-CoV and MERS-CoV originated in bats, with further both circulating in civet cats and camels, respectively. The reservoir for SARS-CoV-2 is not well known, though pangolins and bats are believed to be the source. In fact, a lot is known about the dynamics of SARS-CoV and MERS-CoV, which contributed to contain and control the associated diseases. On the contrary, the current knowledge on the dynamics and clinical aspects (*e.g.* immune response) of SARS-CoV-2 is quite scarce. In the Refs. [4,6,7], relevant similarities and differences are provided between SARS-CoV, MERS-CoV and SARS-CoV-2. For convenience, we give Table 1 which has

* Corresponding author.
E-mail address: Jean.Lubuma@up.ac.za (J.M.-S. Lubuma).

https://doi.org/10.1016/j.mbs.2020.108441

Available online 4 August 2020

Table 1
Most relevant clinical and nonclinical similarities and differences between SARS-CoV, MERS-CoV and SARS-CoV-2.

Similarities & differences	Characteristics	SARS-CoV	MERS-CoV	SARS-CoV-2
Most relevant clinical	Target receptors	ACE-2		ACE-2
	N protein	IFN-λ inhibitor		Unknown
	Chest X-ray	Ground glass opacities		Bilateral, multilobar ground glass opacities
	Chest CT scan	Lobar consolidation Nodular opacities		No nodular opacities
	Transmission	Contact with infected individual	Contact with infected individual	Contact with infected individual
	Reproduction number	0.4	3	1.4–3.0
	Case fatality rate	9.6%	35%	2.3% (4%: 23 July 2020)
	Prevention	Hand hygiene, cough etiquette	Hand hygiene	Hand hygiene cough etiquette
Other relevant	Animal reservoir	Bats and civet cats	Bats and camels	Bats, Pangolins, *etc*
	Number of countries with infected cases	26 Countries	27 Countries	215 Countries
	Countries of emergence	China	Jordan & Saudi Arabia	China
	Date of emergence	November, 2002	September, 2012	December, 2019
	Symptoms	flu-like coughing & fever	flu-like coughing & fever	shortness of breath coughing & fever

more comparative facts than the table in [6] that deals with clinical similarities and differences.

However, it is believed that the novel SARS-CoV-2 is a highly diffusible virus, spread by droplets, *via* direct and indirect transmissions as follows: (a) direct contact with infectious individuals and (b) indirect contact with contaminated objects. In the current situation of absence of a rapid diagnostic test, a safe and effective vaccine or antiviral treatment, the main control measures against the pandemic are social-distancing, standard hygiene practice (*e.g.*, using an alcohol-based sanitizer, washing hands often with soap), wearing a face mask, quarantine and isolation of individuals feared exposed to or diagnosed with coronavirus [1,8–10].

The clinical symptoms of COVID-19 include fever, cough, shortness of breath, acute pneumonia, expectoration, hemoptysis often followed by renal failure [1,11,12]. The incubation period was estimated to be 5.2–5.5 days [13], and the serial interval (the time between the successive onset of symptoms in a chain of transmission) was 7.6 days [1,12]. Since the flu season is about to begin in South Africa, there would be more challenges in distinguishing (and characterizing) the burdens of the two diseases. The scale of COVID-19 is much higher and beyond expectation as compared to SARS and MERS. The World Health Organization (WHO) is concerned with, among others, filling the gaps in understanding of the degree of transmissibility between people, possibility of "super-spreaders" and potential for sustainable person-to-person transmission and spread [1,14]. Super-spreaders are those who transmit the virus to more than 20 patients, and have underlying respiratory diseases with a severe cough [1].

Mathematical modeling has, historically, been used to study the transmission dynamics of infectious diseases, and to assess various control and mitigation strategies. This dates far back to the pioneering works of the likes of Bernoulli [15], Kermack–McKendrick [16], Macdonald [17], Ross [18], *etc.* In particular, mathematical modeling is a useful tool for providing realistic insight into the transmission dynamics and control of rapidly spreading infectious diseases such as COVID-19. A number of models have been designed and used to study the dynamics of the prior two cousins of COVID-19 (SARS and MERS) in Hong Kong [19,20], Singapore [19,21], Beijing [22], China [23], and Middle East [10,24]. In the same vein, another deterministic model was designed to analyze the MERS-CoV outbreak in the Republic of Korea [1,20]. The impact of the timing of control measures associated with a reduction of the transmission rate and diagnostic delays on the outbreak size and duration was also assessed [24]. Simulation of the model reveals that the lack of personal hygiene and targeted control measures were the reasons of the outbreak spread quickly. However, it was reported that strengthening personal hygiene ability of susceptible and quickly isolating or monitoring close contacts are effective measures to control the disease [1]. Furthermore, partial correlation analysis shows that the infectivity and proportion of the asymptomatic infected cases have much influence on the disease spread [25].

Since its emergence in December 2019, numerous models have been designed and used to determine effective ways to combat the pandemic [11,13,26–31]. In particular, Muzimoto and Chowell [29] designed a mathematical model to study the changes in COVID-19 transmission potential in the Diamond Princess Cruises Ship, 2020, as the outbreak progressed. Ferguson et al. [11] used an agent-based model to investigate the impact of non-pharmaceutical interventions (NPIs) to reduce COVID-19 mortality and healthcare demand. Eikenberry et al. [13] proposed mathematical models to assess the potential impact of face masks used by the general public to curtail the COVID-19 pandemic. Finally, Ngonghala et al. [30] presented a mathematical model to assess the potential impact of non-pharmaceutical interventions on curtailing the 2019 novel Coronavirus.

The distinguishing aspect of the current work is the emphasis on the COVID-19 dynamics in South Africa, a country which, though being the top economy of the African continent, is the current epicenter of COVID-19 in Africa. It suffers the usual socio-economic challenges and public health disparities associated with crowded family homes, economic and healthcare inequalities, and variability of the public health responses administered by various provinces. As of 20 July, 2020, South Africa recorded a total of 364,324 confirmed COVID-19 cases and 5033 deaths, which represent 51% and 33% of the respective numbers (*i.e.* 721,292 and 15,170) on the entire African continent [1].

South Africa's National Institute for Communicable Diseases (NICD) confirmed South Africa's first proven case of COVID-19 on 5 March, 2020. Since then, the Government of South Africa has mounted vigorous and effective nationwide response to effectively curtail COVID-19 (see [32] for main steps and dates). Specifically, a National State of Disaster was declared on 15 March, 2020. A travel ban, from and to high-risk countries, was imposed and schools were immediately closed. This was followed (on 26 March, 2020) by a nationwide lockdown structured in five descending alerts starting from extreme restrictions on movement and economy activity (Alert 5) to complete lift of the lockdown (Alert 1). The country is currently at Alert 3 (*i.e.,* greater relaxing of restrictions), after the earlier lowering of the lockdown to Alert 4 (*i.e.* retains most of the restriction of Alert 5) that lasted the entire May of 2020. Of great importance, right at the beginning of the crisis, is the fact that the entire Government established COVID-19 Solidarity Fund, and injected a stimulus of ZAR 500 billion

(*i.e.* US$ 28 billion) representing 10% of South Africa's Gross Domestic Product (GDP). This massive investment enabled South Africa's Government to conduct an effective program of education of the population for compliance, and to implement existing non-pharmaceutical control measures, while strengthening the recovery strategy of the economy and providing support to those who suffer the most during the lockdown.

Despite the efforts mentioned above, there are challenges, particularly in the highly recommended strategy of conducting tests [33], where South Africa is still not meeting its target of 36,000 tests *per* day as set in [34]. Furthermore, over the past two months the number of COVID-19 cases and deaths have been increasing in a worrying manner in South Africa, *viz.* [1,35]: 364,324 cumulative total confirmed cases and 5033 fatalities (20 July 2020) versus 5647 cases and 103 fatalities (1 May, 2020). The breakdown is particularly alarming for the Western Cape, Gauteng and Eastern Cape provinces that have been classified as hotspots or epicenters of the COVID-19 [9]. These factors and challenges motivate the current study. We construct a deterministic model for the transmission dynamics and control of the COVID-19 pandemic in South Africa, taking into account the protocols and the guidelines for isolation, modeling and environmental health [36–38], as designed and followed by South Africa's Government and the National COVID-19 Command Council [9]. Specifically, our model is designed to assess the impact of control measures, such as social-distancing and isolation strategies, against the spread of the disease in South Africa.

The remaining part of the paper is organized as follows. The model is formulated in Section 2. Section 3 is devoted to "materials and results", including estimation of the parameters and some analytical results (such as the asymptotic stability of the continuum of disease-free equilibria of the model and the computation of the final size relations of the COVID-19 model). Section 4 provides numerical simulations, analyses and discussions regarding the epidemiological dynamics of the infection and the impact of available control measures. Finally, conclusions are provided in Section 5.

2. Model formulation

The total human population at time t, denoted by $N(t)$, is divided into six mutually-exclusive compartments, namely susceptible $S(t)$, exposed $E(t)$, asymptomatic infectious $A(t)$, symptomatic infectious $I(t)$, isolated/hospitalized $J(t)$, and recovered individuals $R(t)$. Thus,

$$N(t) = S(t) + E(t) + A(t) + I(t) + J(t) + R(t).$$

This sub-division of the total population is consistent with South Africa's guidelines for isolation from COVID-19 exposure and infection, which states that: 'Though isolation is reserved for persons who are already sick and/or have tested positive for COVID-19 infections, it may in the context of the COVID-19 pandemic, include [38]:

- Isolation at a personal home known as self-isolation. This is the preferred option, subject to the person meeting the self-isolation criteria.
- Isolation in a health facility or at a designated isolation facility. People who cannot self-isolate at home should be considered for admission to such a facility.'

As far as the compartments of human populations are concerned, we use an extension of the standard $SEIR$ model [16], modified by the incorporation of the A and J classes to account for asymptomatic transmission and isolation/hospitalization. However, research works [1,37,39,40], specifically the recent study in [39] which shows that infected patients shed SARS-CoV-2 in their stool, suggest that COVID-19 can be transmitted indirectly following contact with contaminated environment. This is the essence of the campaign to disinfect objects, surfaces, buttons, hands, knobs and places touched often [37]. Although the recent study [41] tends to minimize transmission through contaminated environment, the situation in South Africa is different. Due to crowded family homes and local communities in South Africa, we are more challenged by the following scenario: soon after COVID-19 infected persons cough or sneeze and release droplets from their mouths and noses, people touch objects and surfaces on which these droplets have landed, and then touch their eyes, noses or mouths. Furthermore, the vulnerable situation of South Africa's healthcare facility is a cause for concern about high concentration of the virus in the environments. In this regard, the recent article [42] on the contaminated laundry at Port Elizabeth hospital speaks for itself and motivates the current guidelines in South Africa. For these reasons, we introduce a separate compartment of contaminated environment, $P(t)$. Similar to recent studies [43,44] that regress SARS-CoV-2 sewage measurements onto COVID-19 burden in the population, the class $P(t)$ is relevant in the South African context for one additional reason. That is to isolate SARS-CoV-2 from the 824 Wastewater Treatment Works (WWTW's) across South Africa, to quantify the viral load in the WWTW's, and to build a model that correlates empirical viral load data with COVID-19 confirmed cases in the population. This strategic research project to make environmental surveillance of SARS-CoV-2 a data source is driven by the Centre for Environmental Management at the University of Free State [45].

The population of susceptible individuals is decreased following infection with COVID-19, which can be acquired at the rate (*force of infection*)

$$\lambda = \frac{\beta(t)(\eta_1 A + I + \eta_2 J)}{N} + \beta(t)\eta_3 P,$$

in which the first term expresses direct transmission, while the second term accounts for the indirect (environmental contamination-based) transmission. Here, the parameter $\beta(t)$ is the time-dependent effective contact rate (contact, *per* person *per* unit time, capable of leading to COVID-19 infection). Due to the introduction of social-distancing policy (*e.g.*, lockdown or stay-at-home), it is reasonable to assume that the contact rate will be a decreasing function of time. Unlike the exponential decay function used in [13], we consider the following slow-decaying continuous function $\beta(t)$:

$$\beta(t) = \begin{cases} \beta_0 \ \text{ if } \ t \in [0, \tau_0]. \\ \beta_1 + \dfrac{\beta_0 - \beta_1}{1 + \omega(t - \tau_0)} \ \text{ with } \ \beta_1 \ll \beta_0 \ \text{ if } \ t \geq \tau_0, \end{cases} \tag{1}$$

where τ_0 is the time for the onset of the community lockdown. The parameter $\omega > 0$ is a measure of the compliance of the population with the interventions, mostly the social-distancing, and also the wearing in public of face-masks that has been introduced as of 1 May 2020 in South Africa. The larger ω is, the faster the contact rate $\beta(t)$ decays to β_1, which represents the desired contact rate for COVID-19 to be controlled. Fig. 1 illustrates the profile of the function $\beta(t)$ for different values of ω.

Furthermore, $0 \leq \eta_1 \leq 1$ and $0 \leq \eta_2 \leq 1$ are modification parameters accounting for the assumed reduction in infectiousness of individuals in the asymptomatic (A) and isolated (J) classes, in comparison to infectious individuals in I class. The parameter $0 \leq \eta_3 \leq 1$ is the environmental contamination factor, standing for the *per* capita rate of people who interact with the environment daily. Based on the above, the rate of change of the susceptible population is given by

$$\frac{dS}{dt} = -\lambda S.$$

The population of individuals exposed to SARS-CoV-2 is increased by the infection of exposed individuals (at the rate λ). This population is decreased by the progressing of individuals to the asymptomatic-infectious (at the rate $r\sigma$) and symptomatic-infectious (at the rate $(1 - r)\sigma$) classes, where $0 \leq r \leq 1$ is the proportion of exposed individuals who do not show clinical symptoms of COVID-19 at the end of the incubation period. Hence,

$$\frac{dE}{dt} = \lambda S - \sigma E.$$

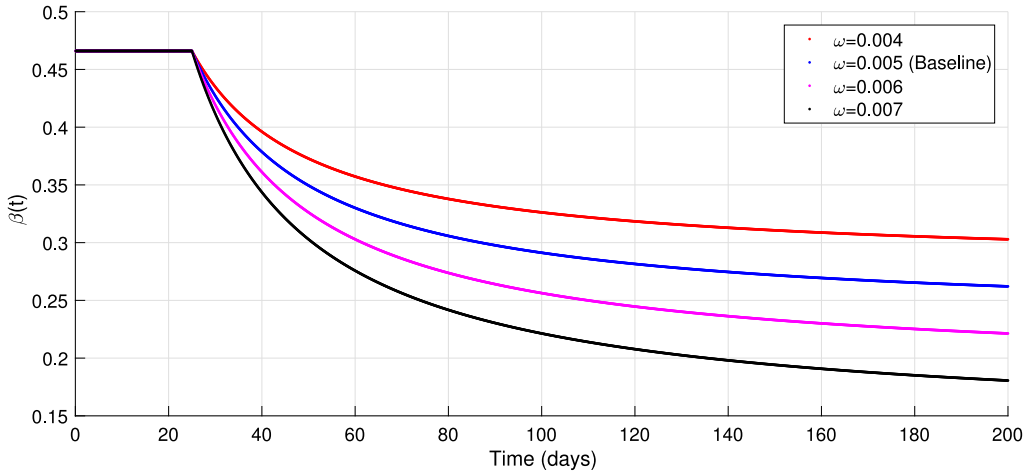

Fig. 1. Profile of the time-varying effective contact rate ($\beta(t)$), as a function of time, for various values of the compliance parameter, ω.

The population of asymptomatic infectious individuals is increased by the progression of infected individuals from the exposed class (at the rate $r\sigma$). It decreases by isolation at the rate γ_1), and by recovery (at the rate τ_1). This gives

$$\frac{dA}{dt} = r\sigma E - (\gamma_1 + \tau_1)A.$$

The population of symptomatic infectious individuals (with clinical symptoms of COVID-19) in I class increases, following the development of clinical symptoms by individuals in the exposed class, at the rate $(1-r)\sigma$. This population decreases by isolation (at the rate γ_2), recovery (at the rate τ_2), and COVID-19 induced mortality (at the rate δ_1). Hence,

$$\frac{dI}{dt} = (1-r)\sigma E - (\gamma_2 + \tau_2 + \delta_1)I.$$

The population of individuals that are isolated or hospitalized ($J(t)$) is generated by the isolation of infectious individuals in the asymptomatic class (at the rate γ_1) and those with clinical symptoms of COVID-19 (at the rate γ_2). It is decreased by recovery (at the rate τ_3) and disease-induced death (at the rate δ_2). Hence,

$$\frac{dJ}{dt} = \gamma_1 A + \gamma_2 I - (\tau_3 + \delta_2)J.$$

The recovered population is generated by the recovery of individuals in A, I and J classes at the rates τ_1, τ_2 and τ_3, respectively. This gives:

$$\frac{dR}{dt} = \tau_1 A + \tau_2 I + \tau_3 J.$$

Infectious individuals in the A, I and J classes contaminate the environment with COVID-19 at the rates ξ_1, ξ_2 and ξ_3, respectively. The virus is cleared from the contaminated environment at the rate υ. Hence,

$$\frac{dP}{dt} = \xi_1 A + \xi_2 I + \xi_3 J - \upsilon P.$$

In summary, the COVID-19 transmission model is given by the following system of nonlinear differential equations (the flow diagram of the model is depicted in Fig. 2, and the associated parameters and state variables are described in Table 2):

$$\begin{aligned}
\frac{dS}{dt} &= -\lambda S,\\
\frac{dE}{dt} &= \lambda S - \sigma E,\\
\frac{dA}{dt} &= r\sigma E - (\gamma_1 + \tau_1)A,\\
\frac{dI}{dt} &= (1-r)\sigma E - (\gamma_2 + \tau_2 + \delta_1)I,\\
\frac{dJ}{dt} &= \gamma_1 A + \gamma_2 I - (\tau_3 + \delta_2)J,\\
\frac{dR}{dt} &= \tau_1 A + \tau_2 I + \tau_3 J,\\
\frac{dP}{dt} &= \xi_1 A + \xi_2 I + \xi_3 J - \upsilon P.
\end{aligned} \tag{2}$$

Like in the case of many other models for COVID-19 [13,30], the model (2) assumes homogeneous mixing, and recovery induced permanent natural immunity against future infections.

The system is solved subject to the following (generalized) nonnegative initial conditions $S(0) \geq 0$, $E(0) \geq 0$, $A(0) \geq 0$, $I(0) \geq 0$, $J(0) \geq 0$, $R(0) \geq 0$, and $P(0) \geq 0$.

Adding the first six equations of the model (2) gives:

$$\frac{dN}{dt} = -\delta_1 I - \delta_2 J. \tag{3}$$

The main novel feature of the model (2) is the incorporation of the important role of SARS-CoV-2 contamination of the environment by infectious individuals in the A, I and J classes. In a number of extensions of the $SEIR$ models for the COVID-19 (*e.g.* [30,46,47]), the approach is to consider models with two or multiple groups depending on risk, age, quarantine or non-quarantine, etc., where each sub-population follows the same transition flows between compartments. The entire South African population being relatively young, and not affected as such by the elderly people-based risk criteria that is used in Europe and North America, we did not consider this approach. Our model also extends in some way, the models in [8,10,48] regarding the transmission dynamics of SARS and MERS diseases.

3. Materials and results

To the question 'will COVID-19 ever disappear?' several sources suggest that the scenario of its complete disappearance is highly unlikely: 'it just transmits too easily in the human population' [49]. As a matter of fact, China and some other countries (including the United States and some European countries) are worried about second waves and new outbreaks [49]. One of WHO's top experts thinks that we might get into a period of cyclical waves or end up with low level endemic disease that we have to deal with (see [49]). The major challenge of suppression of COVID-19 in the absence of vaccine is also echoed in [11]. The above comment suggests that, like [50], we could embark into the full qualitative and quantitative analysis of the model. However, this will be done elsewhere in due course when more is known about the disease. At present, our focus is on the epidemiological dynamics of the infection. This is aligned with the current priority and strategy of the South African Government of mitigation, which focuses on slowing and delaying but not necessarily stopping the epidemic spread, in order to prepare ourselves and be ready with the infrastructure and facility needed by our hospitals and Intensive Care Units (ICUs) when the worse case scenario comes. We will fit the model using South African data and predict the evolution of the epidemic. To this end, we start the next subsection by estimating the epidemiological parameters of the model (2) relevant to COVID-19 data for South Africa obtained from [3].

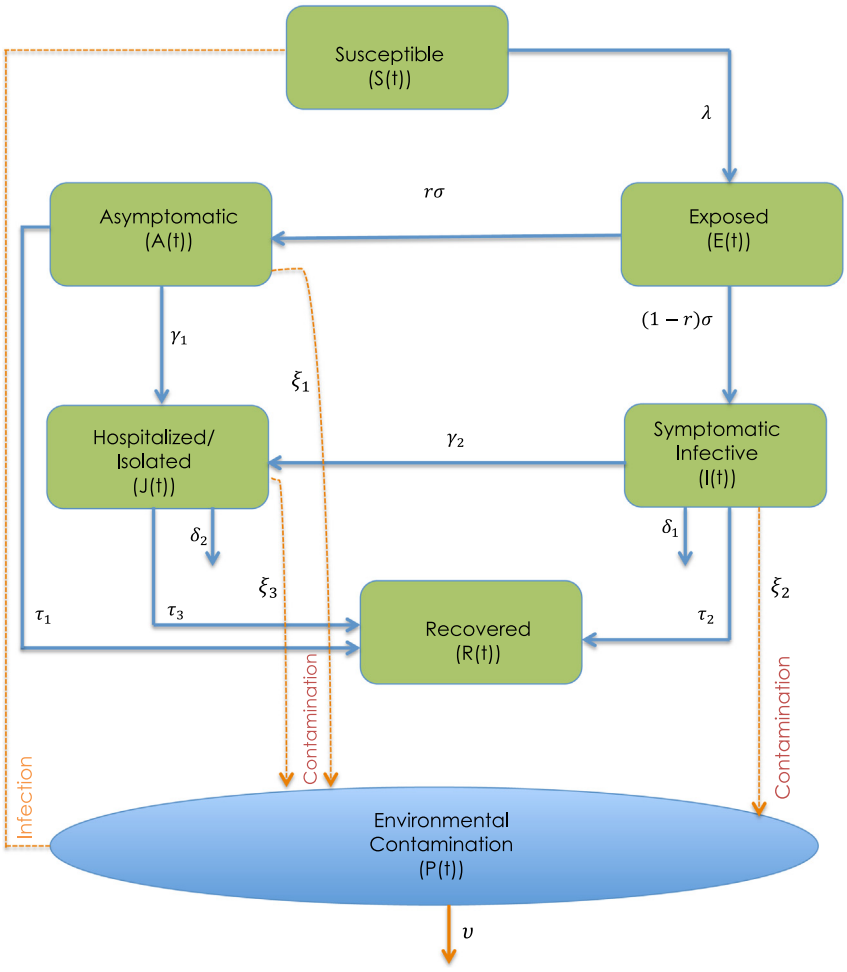

Fig. 2. Flow diagram of the model (2).

Table 2
Description of state variables and parameters of model (2).

Variable	Interpretation
S	Susceptible humans.
E	Exposed humans.
A	Asymptomatic infected humans.
I	Symptomatic infected humans.
J	Isolated/hospitalized humans.
R	Recovered humans.
P	Contaminated environment.
Parameter	**Interpretation**
β	Time-dependent effective contact rate.
β_0	Effective contact rate before the community lockdown.
β_1	Targeted effective contact rate for disease control.
ω	Measure of social-distancing effectiveness.
γ_1 (γ_2)	Isolation rates of asymptomatic (symptomatic) infectious individuals.
η_1 (η_2)	Modification parameters for reduction in infectiousness of asymptomatic (isolated) individuals in comparison to symptomatic infectious individuals.
η_3	The *per* capita rate of people who interact with the environment daily.
τ_0	Starting day of community lockdown.
τ_1 (τ_2) (τ_3)	Recovery rates of asymptomatic (symptomatic) (isolated) infectious individuals.
$r\sigma$ $((1-r)\sigma)$	Progression rates of exposed individuals to asymptomatic (symptomatic) infectious classes.
δ_1 (δ_2)	Disease-induced death rates for symptomatic (isolated) infectious individuals.
ξ_1 (ξ_2) (ξ_3)	Contamination rates of environment by asymptomatic (symptomatic) (isolated) infectious individuals.
υ	Decay or clear rate of the virus on the environment.

3.1. Estimation of parameters and model fitting

National Institute for Communicable Diseases (NICD) confirmed South Africa's first proven (index) case of COVID-19 on 5 March 2020, which we consider to be the first day of the disease. A National State of Disaster was declared on 15 March 2020, followed by a nationwide lockdown from 26 March 2020. We, therefore, take the time of the onset of the lockdown measures in South Africa to be $\tau_0 = 25$.

By fitting the model (using mortality data), we take the effective contact rate $\beta = \beta_0$ before the lockdown to be 0.492 *per* day. The desired minimum contact rate β to which the contact rate should decay is fitted to be $\beta = \beta_1 = 0.166$ *per* day (so as to achieve the target of bringing the control reproduction number to a value below unity). Since the incubation period for COVID-19 ranges from 5–6 days [30], with about 70% of exposed individuals becoming infected, we assume the rate at which exposed individuals become asymptomatically infectious to be $r\sigma = 0.6$ *per* day, so that the rate at which exposed individuals becomes symptomatic is $(1-r)\sigma = 0.4$ *per* day. It should be noted that determining the portion associated with the spread of COVID-19 by asymptomatic individuals is a challenge, as highlighted in [25,51]. It is assumed that there is a short time period of about 5–7 days between the onset of the disease symptoms in the asymptomatic class [30]. Hence, we set the isolation rate of asymptomatic individuals (γ_1) to be $\gamma_1 = 0.85$ *per* day and the isolation rate of symptomatic infected individuals (γ_2) is set to be $\gamma_2 = 1/5$ *per* day. NICD, South Africa [9], estimated the infection period for COVID-19 to range from 6–14 days, so we set the rates at which asymptomatic, symptomatic infectious and isolated individuals recover from COVID-19 (τ_1, τ_2 and τ_3) to be $\tau_1 = 1/6$, $\tau_2 = 1/10$ and $\tau_3 = 1/14$ *per* day, respectively.

While some studies assumed the modification parameters (η_1 and η_2) for the relative infectiousness of asymptomatically infectious individuals in comparison to symptomatically infectious individuals to be $\eta_1 = 0.5$ *per* day [11,30], other studies [52] estimated the parameter to be in the range [0.42, 0.55]. Hence, we set modification parameters η_1 and η_2 to be $\eta_1 = 0.75$ and $\eta_2 = 0.50$ *per* day, respectively. Since data suggest that the COVID-19 case fatality rate in South Africa is about 0.025% [9], we assume the COVID-19 induced-death rates (δ_1 and δ_2) to be $\delta_1 = 0.035$ and $\delta_2 = 0.018$ *per* day.

Contaminated environment is reported to be a substantial route for the transmission of SARS-CoV-2. This is the essence of the campaign to disinfect surfaces, buttons, hands, knobs and other places touched often, apart from scientific reports such as [37,39,40]. The situation requires special attention in South Africa because of the crowded family homes and local communities, which expose people to touch infected objects and surfaces shortly after droplets from COVID-19 infected people have landed there. In fact, in South Africa, a number of hospitals have been closed and the scaling down of the nation-wide lockdown from alert 5 to alert 3 is subjected to schools and other facilities being thoroughly disinfected, as prevention measure to the fact that SARS-CoV-2 survives on surfaces such as plastics and stainless steel for 3–7 days, and from 3 hours to 2 days on wood [53]. Furthermore, the recent studies [43,44] suggest that the presence of SARS-CoV-2 RNA can be detected in sewage weeks (*e.g.* 12–16 days) before the first confirmed case of COVID-19 in the population. Therefore, we estimate the rate υ at which the virus remains infective in the environment before decaying to be 0.85 *per* day, while the shedding rates ξ_1, ξ_2 and ξ_3 of all infectious individuals will be fitted in the range (0, 0.5) virus *per* day *per* individual. Finally, we will fit the value of η_3, the *per* capita rate of people who interact with the environment daily, such that it lies in the range $(0, 0.33]$.

The cumulative number of disease-induced deaths denoted by $D = D(t)$ will be estimated from the following differential equation that results from recording death contributions in the model (2):

$$\frac{dD}{dt} = \delta_1 I + \delta_2 J. \tag{4}$$

We now fit the model (2) using data obtained from [3] for South Africa for the period of three months (21 March to 29 June 2020). Given the inability to realistically measure the size of the asymptomatically-infectious pool, which makes most of COVID-19 case data suspect, we chose to fit the model with the mortality data (which is more reliable). The estimated, assumed and fitted parameters are tabulated in Table 3 (see Table 5 for some sensitivity analysis). Fig. 3 shows a reasonably good fit for total actual deaths and those predicted by the model (2) and Eq. (4).

Table 3
Parameter values for the model (2).

Parameter	Nominal value	Reference
β_0	0.492 (0.002–0.75) *per* day	Fitted
β_1	0.166 (0.002–0.3) *per* day	Fitted
ω	0.005 [0–1/7) *per* day	Fitted
η_1	0.75 (0, 1) *per* day	[30,52]
η_2	0.5 (0, 1) *per* day	[11,30,52]
η_3	$2\times10^{-6}(0, 0.33]$ *per* day *per* individual	Assumed
γ_1	0.85 (0.01, 0.99) *per* day	[30]
γ_2	0.2 (0.01, 0.5) *per* day	[30]
σ	1 (0,1] *per* day	[30]
r	0.6 (0,1) *per* day	Assumed
τ_1	1/6 (0,1) *per* day	[30]
τ_2	1/10 (0,1) *per* day	[30]
τ_3	1/14 (0,1) *per* day	[30]
δ_1, δ_2	0.035, 0.018 (0.01, 0.06) *per* day	[11,30]
ξ_1, ξ_2, ξ_3	0.002, 0.002, 0.001 (0, 0.5) virus *per* day *per* individual	Fitted
υ	0.85 (0.4, 1) *per* day	Assumed

3.2. Analytical results

By separation of variables and integrating factor techniques used sequentially from the first to the last equation in system (2), it follows that any solution of the system corresponding to nonnegative initial conditions is nonnegative. Furthermore, Eq. (3) shows that the total population of human individuals, $N(t)$, is a decreasing function, so that $N(t) \le N(0)$. Thus, by Gronwall inequality, any solution of system (2) belongs to the compact set

$$\Omega = \left\{ (S, E, A, I, J, R, P) \in \mathbb{R}^7_+ : N \le N_0, P \le \frac{(\xi_1+\xi_2+\xi_3)N_0}{\upsilon} \right\}, \tag{5}$$

whenever $(S(0), E(0), A(0), I(0), J(0), R(0), P(0)) \in \Omega$, and where the constant denoted by N_0 ($N_0 \ge N(0)$) is the total population of South Africa. If a solution of (2) lies outside Ω (*e.g.,* $N(t) > N_0$ and $P(t) > (\xi_1+\xi_2+\xi_3)N_0/\upsilon$ for all $t \ge 0$), it is easy to show that the solution will converge to some point of the closed set Ω. Thus, the model (2) is a dynamical system on the compact set Ω, which is absorbing. Thus, Ω is a biologically-feasible region for the model (2).

The system (2) has a continuum of disease-free equilibrium points given by the following manifold (line):

$$\begin{aligned}[\mathcal{DFE}] &:= \{(S^*, E^*, A^*, I^*, J^*, R^*, P^*) \\ &= (S(0), 0, 0, 0, 0, 0, 0);\ 0 < S(0) = N(0) \le N_0\}. \end{aligned} \tag{6}$$

The linear stability of any disease-free equilibrium $\mathcal{E} \in [\mathcal{DFE}]$ can be established using the next generation operator approach on the system (2). We assume in this subsection that the contact rate β is a constant taking either the maximum value ($\beta = \beta_0$) or the minimum value ($\beta = \beta_1$). This assumption makes sense because in the absence of any interventions, the model (2) reduces to the one with $\beta = \beta_0$, while for t large enough, it behaves like the model with $\beta = \beta_1$ when all interventions are successfully implemented. With $K_1 = \gamma_1 + \tau_1$, $K_2 = \gamma_2 + \tau_2 + \delta_1$ and $K_3 = \tau_3 + \delta_2$, the vector $\mathcal{F}$, of new infection terms, and the vector $\mathcal{V}$, of the linear transfers out of and into the infected compartments, are given, respectively, by

$$\begin{aligned} \mathcal{F} &= \left[(\beta S(\eta_1 A + I + \eta_2 J)/N) + \beta S \eta_3 P,\ 0,\ 0,\ 0,\ 0\right]^T, \\ \mathcal{V} &= \left[\sigma E, K_1 A - r\sigma E, K_2 I - (1-r)\sigma E, K_3 J - \gamma_1 A \right. \\ &\quad \left. - \gamma_2 I, \upsilon P - \xi_1 A - \xi_2 I - \xi_3 J\right]^T. \end{aligned}$$

The Jacobian matrices F of $\mathcal{F}$ and V of $\mathcal{V}$ are computed at the point $\mathcal{E}$ with respect to the infectious classes (E, A, I, J, P). It follows from [54] that the control reproduction number of the model (2) denoted by $\mathcal{R}_c$, is given by $\mathcal{R}_c = \rho(FV^{-1})$, where $\rho(.)$ is the spectral radius of the next generation matrix FV^{-1}.

Simple computations show that $\mathcal{R}_c$ can be rewritten as the sum of two main contributions (*viz.* humans and environment) as follows:

$$\mathcal{R}_c = \mathcal{R}_c^{hh} + \mathcal{R}_c^{env}, \tag{7}$$

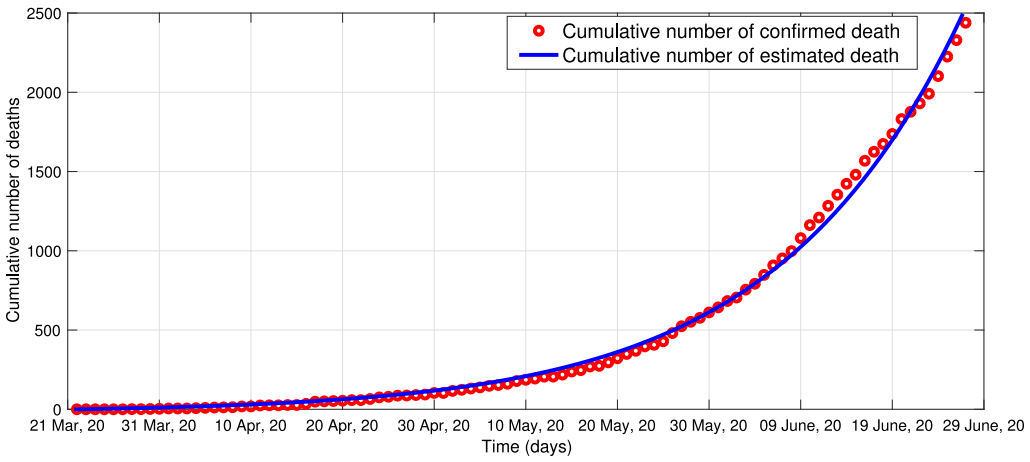

Fig. 3. Time series plot showing a least square fit of Eq. (4) coupled with system (2), using South Africa COVID-19 reported cases for cumulative number of deaths. Parameter values used are as given in Table 3.

Table 4
Estimate of COVID-19 effective reproduction numbers ($\mathcal{R}_e(t)$) for some countries.

Country	Estimate effective reproduction number $\mathcal{R}_e(t)$	Reference
Hubei Province, China	6.49 (6.31, 6.66)	[55]
Spain	5.17 (4.98, 5.37)	[28]
United States	3.29 (3.15, 3.43)	[28]
Canada	2.30 (2.07, 2.57)	[28]
United Kingdom	2.90 (2.72, 3.10)	[28]
Italy	2.44 (2.41, 2.47)	[28]
Germany	3.29 (3.18, 3.40)	[28]
France	3.09 (2.99, 3.19)	[28]
South Africa	2.2 (2.1, 2.8)	[9]

where,

$$\mathcal{R}_c^{hh} = \frac{\beta\left[rK_2(K_3\sigma_1+\gamma_1)+(1-r)K_1(K_3\eta_2+\gamma_2)\right]}{K_1K_2K_3}\frac{S(0)}{N(0)}, \tag{8}$$

$$\mathcal{R}_c^{env} = \frac{\beta\eta_3 S(0)\left[rK_2(K_3\xi_1+\gamma_1\xi_3)+(1-r)K_1(K_3\xi_2+\gamma_2\xi_3)\right]}{K_1K_2K_3\upsilon}\frac{S(0)}{N(0)}. \tag{9}$$

It should be mentioned that we do not make the substitution $S(0)/N(0) = 1$ in order to link the control reproduction number $\mathcal{R}_c$ to the effective reproduction number introduced in Remark 2 below.

The threshold quantity $\mathcal{R}_c$ measures the average number of new COVID-19 cases that one infected case can generate if introduced into a population where basic public health interventions (such as isolation, social-distancing etc.) are implemented [30]. Using Theorem 2 in [54], the following result is established.

Theorem 1. *Each point $\mathcal{E}$ in the continuum $[D\mathcal{FE}]$ of disease-free equilibria of the model (2) is locally-asymptotically stable if $\mathcal{R}_c < 1$.*

Remark 2. The system (2) is non-autonomous due to the time-dependent contact rate, $\beta(t)$. It could, therefore, be appropriate to consider the effective reproduction number $\mathcal{R}_e(t)$ defined as the expected number of secondary cases produced by one typical infectious individual joining in a population during its infectious period. Notice that $\mathcal{R}_e(t)$ quantifies the instantaneous transmissibility of the disease. The effective reproduction number can be estimated by applying the next generation matrix approach in [54]. In doing so, the expression of $\mathcal{R}_e(t)$ is similar to Eqs. (7)–(9) where β, $S(0)$ and $N(0)$ are replaced by $\beta(t)$, $S(t)$ and $N(t)$, respectively.

The effective reproduction numbers for some countries with COVID-19 cases are given on Table 4 as of 13 March 2020.

Remark 3. The epidemiological implication of Theorem 1 is that COVID-19 can be eliminated from the population when $\mathcal{R}_c < 1$, provided that the initial sizes of the sub-populations of the model are in the basin of attraction of the said DFE, $\mathcal{E}$. Here, the ideal situation $\mathcal{R}_c < 1$ does not happen, as mentioned earlier and seen from Table 4. For instance, consider the disease-free equilibrium $\mathcal{E} \in [D\mathcal{FE}]$ corresponding to $S(0) = N(0)$. Using the set of parameter values in Table 3, with $\beta = \beta_0 = 0.492$, we estimated the value of the control reproduction number for South Africa to be $\mathcal{R}_c = 2.9562$. However, we obtained $\mathcal{R}_c = 0.9974$ for the case when $\beta = \beta_1 = 0.166$. Hence implementing, for a sufficiently long period of time, population-wide social-distancing (lockdown) combined with other strict interventions such as self-isolation of cases and wearing of face-masks, has the potential to bring the control reproduction number below unity and thus to suppress transmission, as suggested in the reference [11]. We show below that for an epidemic model such as model (2), the continuum of disease-free equilibria is both a stable set and a global attractor.

Theorem 4. *If $\mathcal{R}_c < 1$, then the continuum of disease-free equilibria of the model (2) is globally asymptotically stable in the positively-invariant and absorbing compact set Ω defined in (5).*

Proof. It was proved that the system (2) is a dynamical system in the biologically feasible region Ω which contains the set $[D\mathcal{FE}]$. Define on Ω the candidate Lyapunov function:

$$\mathcal{L} = E + a_0A + a_1I + a_2J + a_3P,$$

where the positive constants a_0, a_1, a_2, a_3 will be determined shortly. Then the directional derivative $\dot{\mathcal{L}}$ (where a dot represents derivative with respect to t) of $\mathcal{L}$ in the direction of the vector-function defined by the right-hand side of the system (2), (*i.e.* the derivative along the trajectories), is given by

$$\begin{aligned}\dot{\mathcal{L}} &= \lambda S - \sigma E + a_0r\sigma E - a_0K_1A\\ &+ a_1(1-r)\sigma E - a_1K_2I + a_2\gamma_1A + a_2\gamma_2I - a_2K_3J\\ &+ a_3(\xi_1A + \xi_2I + \xi_3J - \upsilon P).\end{aligned}$$

Since $S/N \le 1$ and $S \le N_0$ in Ω, some lengthy computations lead the following estimate of $\dot{\mathcal{L}}$:

$$\begin{aligned}\dot{\mathcal{L}} &\le \left[a_1(1-r)\sigma + a_0r\sigma - \sigma\right]E + \left[\beta\eta_1 - a_0K_1 + a_2\gamma_1 + a_3\xi_1\right]A\\ &+ \left[\beta + a_2\gamma_2 + a_3\xi_2 - a_1K_2\right]I + \left[\beta\eta_2 + a_3\xi_3 - a_2K_3\right]J\\ &+ \left[\beta\eta_3N_0 - a_3\upsilon\right]P.\end{aligned}$$

The constants $a_0 > 0, a_1 > 0, a_2 > 0, a_3 > 0$ and $a_4 > 0$ are then chosen to be the unique solution of the following algebraic system:

$$\begin{cases} \beta\eta_1 - a_0K_1 + a_2\gamma_1 + a_3\xi_1 = 0, \\ \beta + a_2\gamma_2 + a_3\xi_2 - a_1K_2 = 0, \\ \beta\eta_2 + a_3\xi_3 - a_2K_3 = 0, \\ \beta\eta_3N_0 - a_3\upsilon = 0. \end{cases}$$

This simplifies the above estimate of $\dot{\mathcal{L}}$ into

$$\dot{\mathcal{L}} \leq -\sigma(1 - \mathcal{R}_c)E, \tag{10}$$

where the control reproduction number is given in (7).

Assume, from now on, that $\mathcal{R}_c < 1$. Then, it follows from (10) that

$$\dot{\mathcal{L}} \leq 0, \text{ with } \dot{\mathcal{L}} = 0 \text{ if and only if } E = 0. \tag{11}$$

Consider the set $\mathcal{M}$ defined by

$$\mathcal{M} = \{(S, E, A, I, J, R, P) \in \Omega : \dot{\mathcal{L}} = 0\}$$

and let $\mathcal{B}$ be a compact invariant set contained in $\mathcal{M}$. Denote by $S(t)$, $E(t)$, $A(t)$, $I(t)$, $J(t)$, $R(t)$ and $P(t)$ the solution of the system (2) initiated at a point $B \in \mathcal{B}$. It is easy to show that $(S(t), E(t), A(t), I(t), J(t), R(t), P(t)) \in \mathcal{M}$ which, by (11) and (2), implies that $(S(t), E(t), A(t), I(t), J(t), R(t), P(t)) \in [\mathcal{DFE}]$. Since B and $\mathcal{B}$ were taken arbitrarily, we have shown that the largest compact invariant set contained in $\mathcal{M}$ is the set $[\mathcal{DFE}]$. It follows, from LaSalle's Invariance Principle [56], that the set $[\mathcal{DFE}]$ of equilibria of the system (2) is globally asymptotically stable in Ω. ■

Though each disease-free equilibrium point $\mathcal{E} \in [\mathcal{DFE}]$ of the model (2) is locally asymptotically stable when $\mathcal{R}_c < 1$, the above result shows that the continuum (set) $[\mathcal{DFE}]$ is globally asymptotically stable under this condition (thus, COVID-19 will be effectively controlled or eliminated from the population).

With the expression of the control reproduction number computed in (7) for the constant contact rates $\beta = \beta_0$ and $\beta = \beta_1$, we are in a position to state an important result on the final sizes of the COVID-19 pandemic variables. The result provides a measure of the severity of the epidemic in terms of its final size relations, as done in the study [57] that was recently applied to a COVID-19 model in [30]. The result reads as follows:

Theorem 5. *Denote $N_\infty := \lim_{t\to\infty} N(t)$ and $S_0 \equiv S(0)$. Let x denote the column vector $x := (E,\ A,\ I,\ J,\ P)^T$ and let b be the row vector defined by $b := \left(0,\ \eta_1,\ 1,\ \eta_2,\ N_0\eta_3\right)$. Then, we have the following:*

1. *The functions $x(t)$, $S(t)$ and $N(t)$ satisfy the properties*

$$\begin{aligned} x_\infty := \lim_{t\to\infty} x(t) = 0 \text{ and } \lim_{t\to\infty} S(t) = S_\infty > 0, \\ \text{so that } 0 < S_\infty \leq N_\infty < N_0, \end{aligned} \tag{12}$$

   where S_∞ is the unknown final size of the epidemic to be determined.
2. *The final size relation for the COVID-19 pandemic is given by*

$$\ln\frac{S_0}{S_\infty} \geq \mathcal{R}_c\left(1 - \frac{S_\infty}{S_0}\right) + \beta b V^{-1} x_0, \tag{13}$$

   where $\beta = \beta_0$ or β_1, $x_0 = x(0)$ and the inverse matrix V^{-1} was used in the computation of $\mathcal{R}_c$.

To simplify the final size relation (13), it is usual to set some of the initial conditions to be equal to zero [30,57]. A typical choice is $E(0) = A(0) = J(0) = P(0) = 0$ and $I(0) > 0$. In this case, by computing the matrix V^{-1}, one obtains the following simpler lower bound for the final size relation (13):

$$\ln\frac{S_0}{S_\infty} \geq \mathcal{R}_c\left(1 - \frac{S_\infty}{S_0}\right) + \beta\left(\frac{1}{K_1} + \frac{\eta_2\gamma_2}{K_2K_3} + \eta_3N_0\right)I(0). \tag{14}$$

For the analysis in the next section, Theorem 5 will be used as follows. The number $\alpha := 1 - \frac{S_\infty}{S_0}$, called the "attack rate or ratio" of the epidemic, is a measure of its severity, apart from the number S_∞ of susceptible individuals who escaped the epidemic [58]. The larger the attack rate is, the more severe the epidemic is, in terms of the cumulative total number $S_0 - S_\infty$ of COVID-19 cases. Furthermore, Theorem 5 highlights a classical result of Kermack and McKendrick [16], namely irrespective of the value of the control reproduction number $\mathcal{R}_c$, the epidemic will die out and stop, but not because of exhaustion of susceptible individuals.

4. Numerical simulations, analysis and discussion

In this section, numerical simulations and epidemiological analysis are carried out using the COVID-19 data for South Africa to assess the potential impact of the available intervention strategies.

4.1. Compliance with social-distancing measures

The effect of social-distancing coupled with other interventions such as isolation is assessed by simulating the model (2) using the baseline parameter values presented in Table 3. The simulations show a decrease in the numbers of exposed, asymptomatic, symptomatic and isolated individuals with increase in the social-distancing parameter ω, as depicted on Fig. 4(A)–(D). This result is consistent with the fact that the social-distancing intervention reduces the number of cases in the USA [30]. Of great importance is also what the same Fig. 4(A)–(D) reveals regarding when to reach the peak of the pandemic in South Africa under the current strict social-distancing protocols. If 6 in 1000 people comply with the interventions *per* day, *i.e.* the social-distancing effectiveness parameter $\omega = 0.006$, then the peak of the pandemic is expected to be attained around April 2021, with 1,000,000 cumulative total confirmed cases at peak time, as seen on Fig. 5(A). On the contrary, if the social distancing is relaxed to a moderate or mild effectiveness level ($\omega = 0.004$) then the cumulative total confirmed cases at the peak of the pandemic will rise to around 2,500,000 (see Fig. 5(A)). Further simulations of the model show that the time to COVID-19 control (or elimination) using strict social-distancing protocol is expected to be attained by March 2022.

It should be noted, here and in what follows, that our projections are consistent with those of South Africa's government modeling consortium [36] in the sense that there are substantial increases in numbers of COVID-19 cases and mortality. However, the increases are more significant in the government's estimates. One explanation of the discrepancy is that the government's estimates are hugely influenced by conducted tests, a parameter that is not incorporated in our model due to challenges with test strategy and changing testing pattern, as acknowledged by the NICD [36].

The simulations presented on Fig. 5 deal with cumulative total numbers of affected individuals. As the social-distancing parameter (ω) increases, items (A), (B) and (C) of Fig. 5 show a decrease in the cumulative numbers of infections, recoveries and deaths, respectively. Fig. 5(D) has a compelling message regarding the scenario were no social-distancing is implemented ($\omega = 0$). That is, the cumulative total number of COVID-19 induced mortality increases significantly with time. Thus, these simulations show that the implementation of strict social-distancing policy (popularly known as lockdown or stay at home) by South Africa's government has a significant community-wide impact in mitigating the transmission of COVID-19.

A further remark is in order about Fig. 5 and the associated compelling message mentioned above. The nationwide lockdown in South Africa, which started on 26 March 2020 at Alert 5 (*i.e.* most stringent restrictions on movement and economy activity) was down-scaled two times as follows: to Alert 4 (*i.e* retains most of the restriction of Alert 5) that lasted from 1–31 May 2020, and to Alert 3 (*i.e.* greater relaxing of restrictions) from 1 June 2020. There is now strong uproar to completely lift the lockdown to Alert 1. The main challenge is, of course, to ensure that any easing of the lockdown measures does not erase the

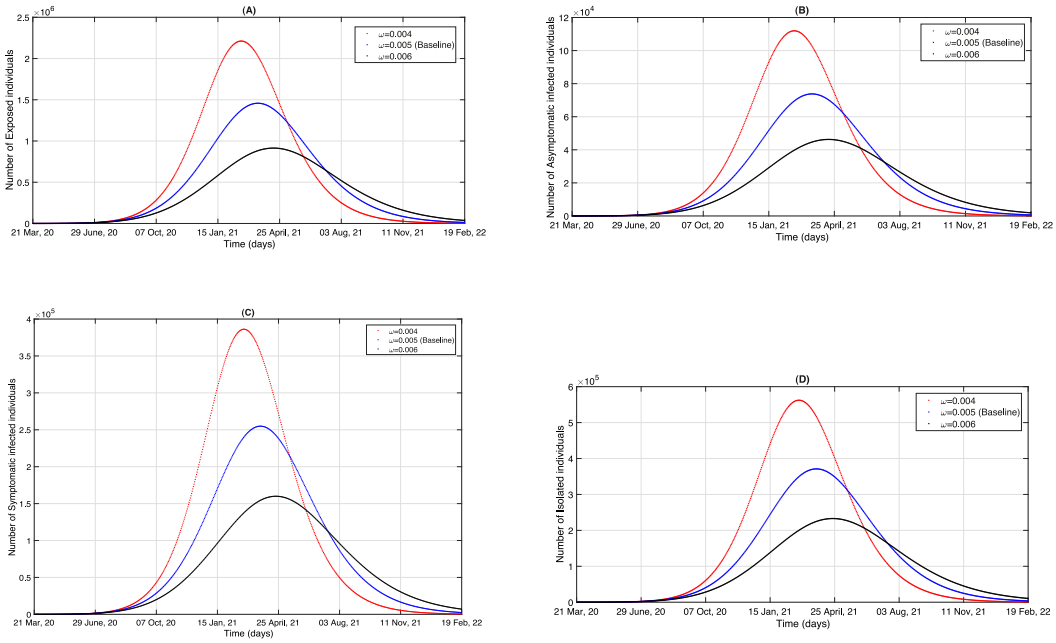

Fig. 4. Simulations of the model (2), showing the decrease in numbers of COVID-19 infected individuals as the social-distancing parameter ω increases: (A) Exposed, (B) Asymptomatic, (C) Symptomatic, and (D) Isolated individuals, respectively. Parameter values used are as given in Table 3 with various values of ω.

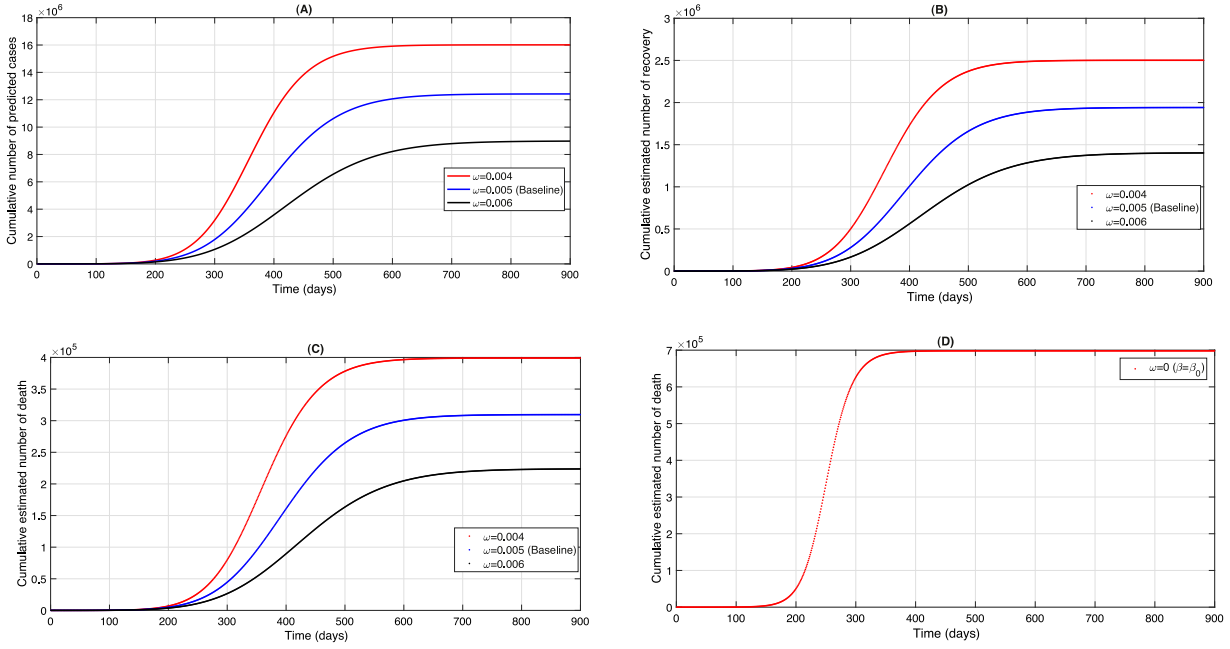

Fig. 5. While the cumulative total number of deaths significantly increases in the absence of interventions *i.e.* $\omega = 0$ (D), there is a decrease in cumulative numbers of carriers of infections (A), recoveries (B), and deaths (D) as ω increases. Parameter values used are as given in Table 3 with various values of the compliance parameter ω.

gains made so far in curtailing the pandemic. Hence, like [30,59], this study strongly suggests that absolute caution should be exercised before terminating the current strict social-distancing protocols or lowering the COVID-19 alerts, so as to avoid the resurgence of the pandemic. Recent findings already showed that certain countries, such as South Korea and Hong Kong, that have relaxed the successfully-implemented social-distancing measures are now experiencing a rebirth of COVID-19 [60]. It is commendable that, recently (12 July 2020), South Africa's government decided to maintain the nationwide lockdown at the current Alert 3 and re-introduced drastic measures such as a curfew from 9 pm to 4 am, while reaffirming its commitment to alleviate the sufferings of the people during lockdown.

4.2. The impact of isolation

The effect of isolation of individuals infected with COVID-19 is monitored by simulating the model (2) using parameter values given in Table 3 with various levels of effectiveness of isolation of asymptomatic (γ_1) and symptomatic (γ_2) infectious individuals. The results obtained, as *per* Fig. 6(A)–(D), show that isolation of infected individuals has a great impact in reducing the number of cases. For instance, Fig. 6(C) suggests that early isolation of infected individuals could lead to averting of 250,000 symptomatic cases *i.e.* a decrease by 45%, thereby reducing disease burden.

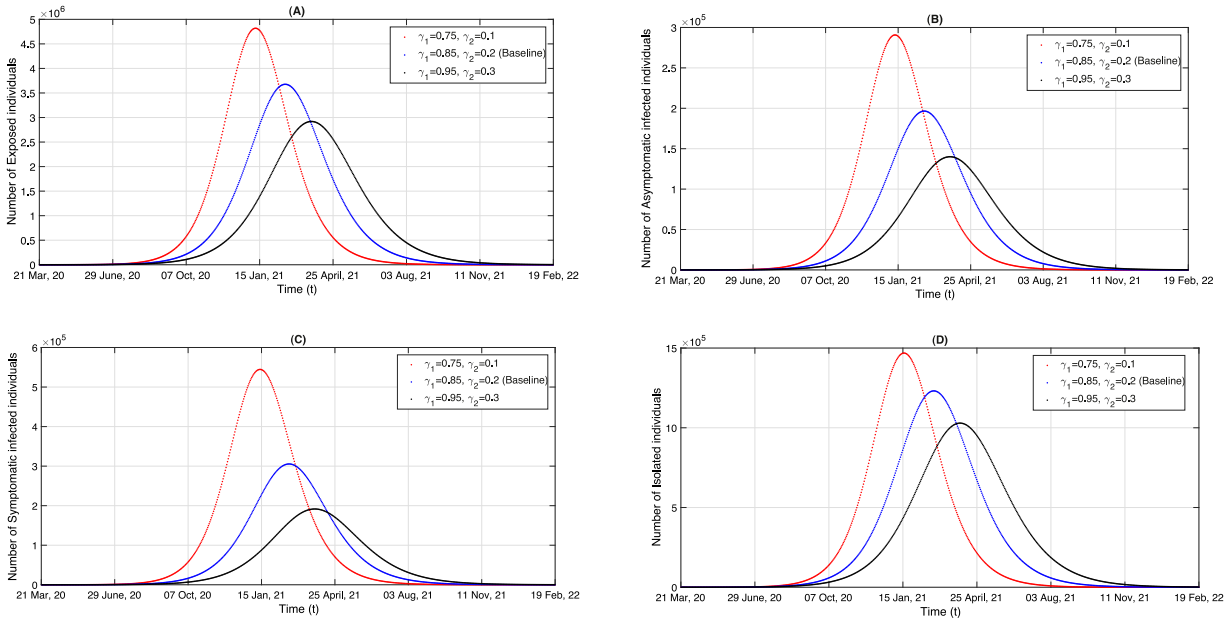

Fig. 6. Simulations of the model (2), showing changes in the numbers of COVID-19 infected individuals, as the isolation rates (γ_1 and γ_2) vary: (A) Exposed, (B) Asymptomatic, (C) Symptomatic, and (D) Isolated individuals, respectively. Parameter values used are as given in Table 3.

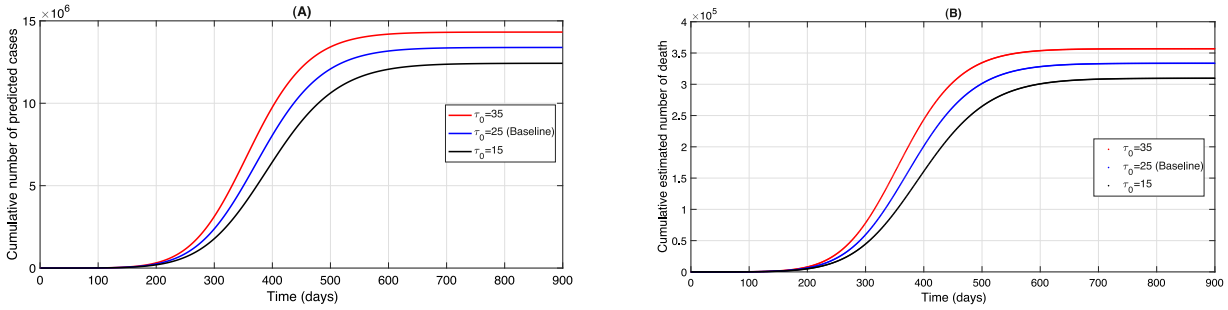

Fig. 7. Simulations of the model (2), showing changes in the cumulative number of COVID-19 affected individuals: (A) Cases and (B) Deaths. Parameter values used are as given in Table 3.

4.3. Impact of starting time of the lockdown

Additional simulations were carried out to assess the population-level impact of early or late implementation of the lockdown policy. Using various values of the lockdown implementation dates (τ_0), Fig. 7(A)–(B) and Fig. 8(A)–(D) deal with cumulative total cases and deaths, respectively. The figures show that the early implementation of strict social-distancing protocols right from the very beginning of the COVID-19 pandemic in South Africa (*i.e.* 25 March 2020), has played an important role in terms of lowering the peak daily cases of COVID-19, as depicted on Fig. 8(A)–(D). The simulation presented in Fig. 7(A) shows that implementation of lockdown by the government ten days earlier has helped in averting 50,000 cases of COVID-19, which represents a 0.4% decrease in number of cases. Furthermore, our simulations showed that the early implementation of social-distancing measures in the country by ten days has significantly decrease cumulative COVID-19 related mortality by about 10,000 (*i.e.* 10% reduction) nationwide as shown on Fig. 7(B).

4.4. Severity of the COVID-19 pandemic

Numerical simulations of the model using the initial conditions $S_0 = 5.9 \times 10^7$ (population of South Africa), $E(0) = A(0) = P(0) = 0$ and $I(0) = 65$ are presented in Fig. 9. In the absence of any control measures, *i.e.* the contact rate is $\beta = \beta_0$, Fig. 9(A) shows that the number of susceptible individuals who will escape COVID-19 at the end of the pandemic is $S_\infty = 0.9 \times 10^7$. In the case when control measures are successfully implemented, so that $\beta = \beta_1$, the final size of susceptible individuals is $S_\infty = 3.50 \times 10^7$, as shown on Fig. 9(B). Furthermore, the computed attack rate (α) for $\beta = \beta_0$ is found to be almost the double of the case when $\beta = \beta_1$, namely $\alpha = 0.8475$ and $\alpha = 0.4068$, respectively. Hence, the final size relation given in Theorem 5, in its simplified form (14), is satisfied since $\mathcal{R}_c = 2.9562$ for $\beta = \beta_0$ and $\mathcal{R}_c = 0.9974$ for $\beta = \beta_1$ (see Remark 3).

These results confirm that the infection is more severe for high contact rate β. Notice that, for the case when $\beta = \beta_0$, the total number of COVID-19 cases at the end of the pandemic is obtained to be $S_0 - S_\infty = 50,500,000$, which is more than three times the number obtained for $\beta = \beta_1$ (15,000,000) (see Fig. 9). Thus, our predictions in terms of infection peak time and corresponding number of cases are consistent with those of South Africa's government [36].

4.5. Impact of environmental contamination

As mentioned earlier, it is widely campaigned that SARS-CoV-2 survives from few to several days on different surfaces (*e.g.* plastic, stainless steel, wood, *etc.*) [53]. In particular, the crowded family homes and local communities in South Africa easily expose people to touching infected objects and surfaces shortly after droplets from COVID-19 infected people have landed there. Therefore, it is not surprising that at the onset of the COVID-19 pandemic in South Africa

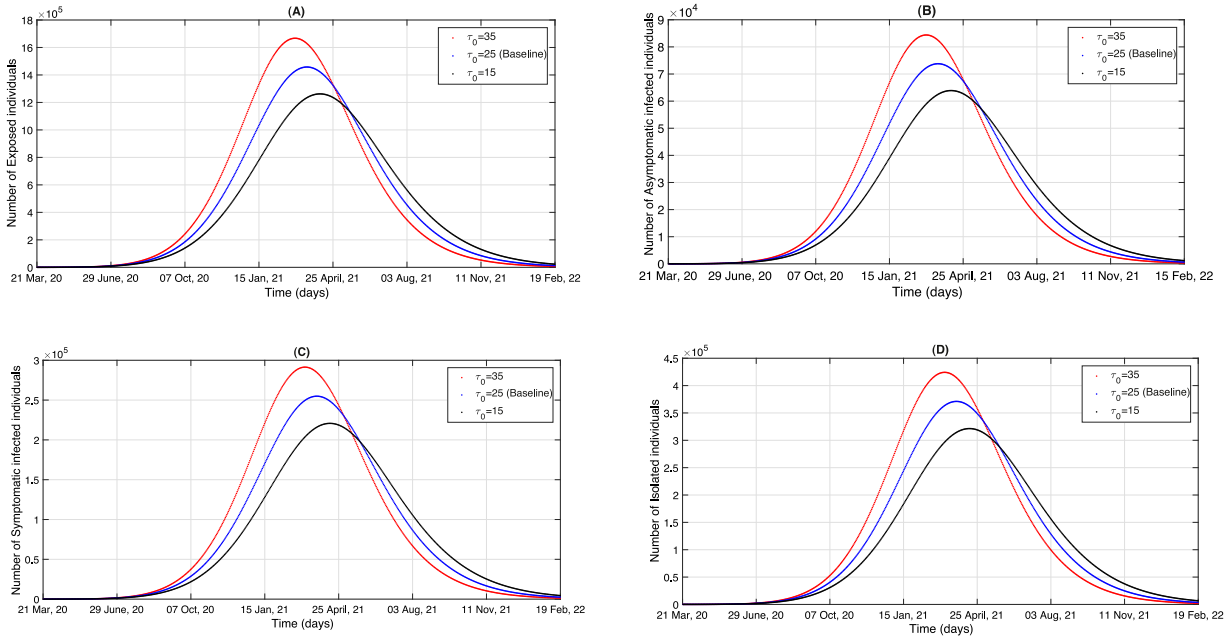

Fig. 8. Simulations of the model (2), showing changes in the number of COVID-19 infected individuals, as the parameter τ_0 for the starting time of the lockdown varies: (A) Exposed, (B) Asymptomatic, (C) Symptomatic, and (D) Isolated individuals, respectively. Parameter values used are as given in Table 3.

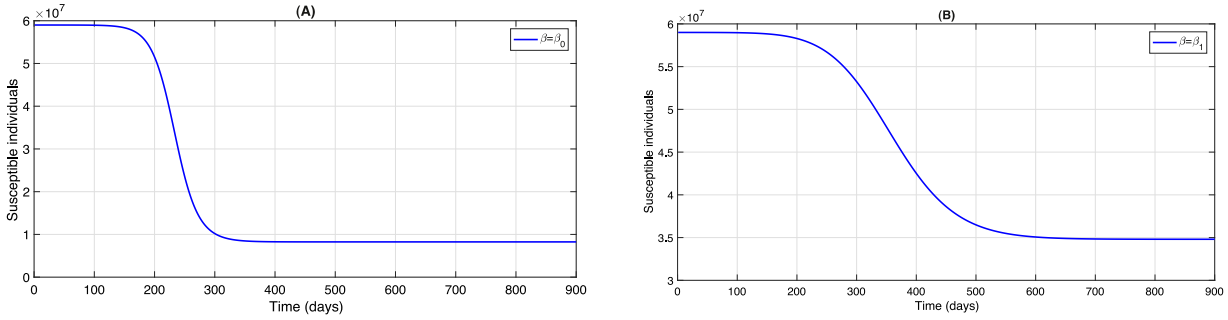

Fig. 9. Simulations of the model (2) for the computation of the final size relations of the COVID-19 pandemic, namely the number S_∞ of susceptible individuals who escaped the epidemic and the attack rate α of the epidemic. (A) In the absence of any control measures ($\beta = \beta_0$). (B) Under strict lockdown ($\beta = \beta_1$). Parameter values used are as given in Table 3, while initial conditions are $S(0) = 59 \times 10^7$, $I(0) = 65$, $E(0) = A(0) = J(0) = P(0) = R(0) = 0$.

where $\beta = \beta_0$ in our model, the environmental contamination has a substantial contribution ($\mathcal{R}_c^{env} = 0.5540$) of 19% to the overall control reproduction number $\mathcal{R}_c = 2.9562$ (See Remark 3). Using data, the study [43,44] correlates SARS-CoV-2 load in sewage with actual COVID-19 cases in a population. A strategic research project on environmental surveillance of SARS-CoV-2 as data source, is underway in South Africa [45].

In the absence of data at present in South Africa, we carried out global sensitivity analysis, using the Partial Rank Correlation Coefficient (PRCC), to determine the most influential parameters for the transmission dynamics of COVID-19 in South Africa. We determined the PRCC values for some parameters of the model (2), using the control reproduction number ($\mathcal{R}_c$) and the total number of infected humans ($I(t) + J(t)$) as the response functions. A total of 1000 simulations (runs) of the model for the Latin Hypercube Sampling (LHS) matrix were then carried out using the parameter baseline values and their ranges as tabulated in Table 3. The parameters with significant negative and positive PRCC values are seen from Table 5. In particular, the environmental transmission factor η_3 and the rate of virus cleaning from the environment (υ) are among the most influential parameters.

In view of the sensitivity analysis described above, the impact of environmental contamination in the transmission is assessed by simulating the model (2) with various values of the transmission rate (η_3) and the virus cleaning rate υ. Notice that, the number of cases increases with increase in the transmission rate η_3, as presented in items (A) and (B) of Fig. 10. On the other hand, when υ becomes larger than the baseline value, items (A) and (B) of Fig. 11 show continued increases in cumulative number of cases and deaths, respectively.

5. Conclusions

Since the beginning of March 2020, South Africa has been hit by the COVID-19 pandemic in a more complex manner than China, where the disease started, as all cases were imported and culminated into challenging types of transmissions of the infection in super-spread events, hotspot transmission areas, community transmission areas, etc. In the absence of treatment and vaccine that could mitigate or eradicate the disease, South Africa's government response to COVID-19 is to flatten the curve of infection early and to reduce the number of infections at the peak time, while expanding our healthcare capacity and better preparing our equipment in hospitals for the worse scenario to come [36].

Based on the authors' experience with the outbreaks of the Severe Acute Respiratory Syndrome (SARS) [8] and the Middle East Respiratory Syndrome (MERS) [10], we have considered, for the transmission dynamics of COVID-19 in South Africa, an extension of the

Table 5
PRCC values of the model: - with the control reproduction number ($\mathcal{R}_c$) as the response function for (A) $\beta = \beta_0$ and (C) $\beta = \beta_1$; - with the total number of infected humans ($I(t) + J(t)$) as the response function for (B) $\beta = \beta_0$ and (D) $\beta = \beta_1$. Parameter values and ranges used are as given in Table 3.

Parameter	β	η_3	γ_1	γ_2	ξ_1	ξ_2	ξ_3	υ
PRCCs - $\mathcal{R}_c$ (A)	−0.182	0.091	0.018	−0.068	−0.062	−0.17	0.015	0.22
PRCCs - Total ($I + J$) (B)	−0.095	−0.15	0.03	0.051	−0.14	−0.075	−0.05	−0.075
PRCCs - $\mathcal{R}_c$ (C)	−0.18	0.098	−0.20	0.035	0.049	−0.005	0.11	0.17
PRCCs - Total ($I + J$) (D)	−0.172	0.11	−0.15	−0.035	−0.03	0.005	0.072	−0.081

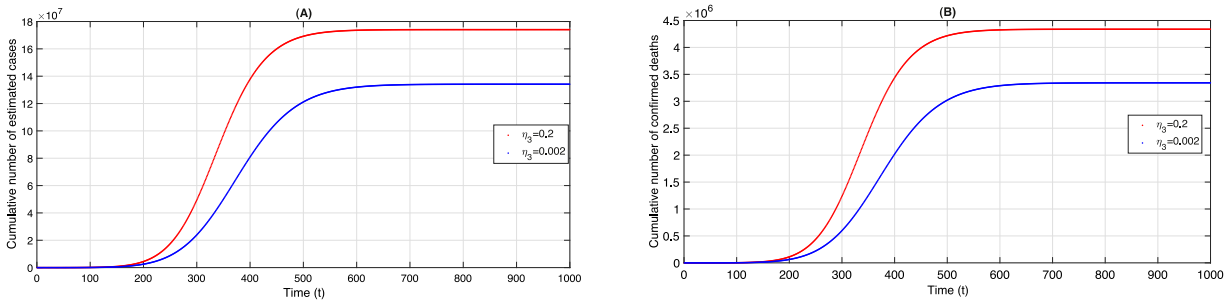

Fig. 10. Simulations of the model (2), showing changes in the cumulative numbers of COVID-19 related cases (A) and deaths (B) as the environmental transmission factor (η_3) changes. Parameter values used are as given in Table 3.

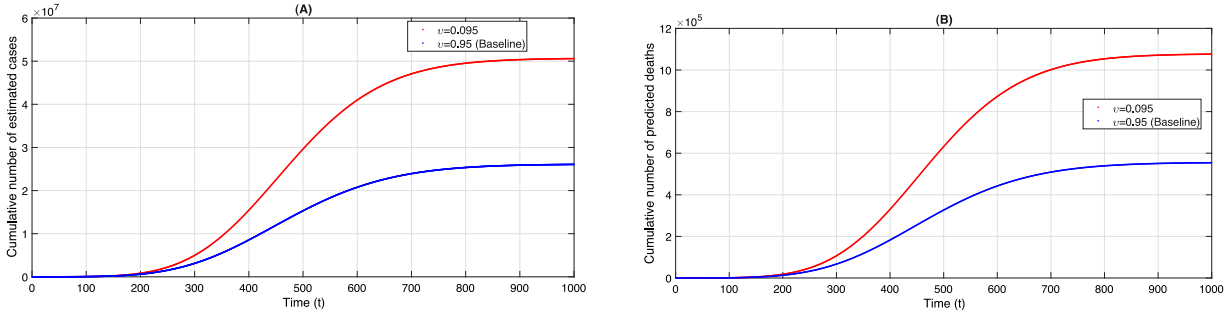

Fig. 11. Simulations of the model (2), showing changes in the cumulative numbers of COVID-19 related cases (A) and deaths (B) as the cleaning rate of virus (υ) in the environment changes. Parameter values used are as given in Table 3.

standard *SEIR* model in which the infected individuals are stratified into Exposed, Asymptomatic, Symptomatic infectious and Isolated/Hospitalized compartments, respectively. We have also added a compartment of contaminated environment, in accordance with the campaign to disinfect surfaces, buttons, hands, knobs and other places touched often [37,53], as well as the correlation of SARS-CoV-2 load in wastewater with COVID-19 cases in the population [43,44]. The model was used to assess the impact of various non-pharmaceutical measures on the control of the pandemic in South Africa [11].

The main findings of the study, which in a nutshell suggest that the COVID-19 pandemic can be controlled in South Africa provided that all the envisaged measures are implemented effectively, include the following:

(I) There is a good fit of the cumulative number of COVID-19-induced deaths with the model system plot.

(II) We introduced a social-distancing effectiveness parameter $\omega > 0$ in terms of which threshold analysis led to the following result: The (cumulative total) numbers of COVID-19 infected individuals (*i.e.* exposed, asymptomatic, symptomatic, and isolated/hospitalized individuals) decrease as ω increases. Furthermore, in the absence of social-distancing (*i.e.* $\omega = 0$), the cumulative total number of COVID-19-induced mortality increases significantly with time.

(III) We introduced a starting time parameter τ_0 for the lockdown measure in terms of which the following result was obtained: Early implementation of the lockdown intervention (i.e. decreasing τ_0) results in considerable decrease in the number of COVID-19 infected individuals. In particular, the COVID-19 pandemic peak time (*i.e.* mid-April 2021 for $\tau_0 = 25$) can be delayed and its peak daily case becomes larger if $\tau_0 > 25$.

(IV) We introduced two parameters, namely η_3 for the environmental transmission and υ for the cleaning rate of virus in the environment. We showed that increasing η_3 kept both numbers of COVID-19 infected and dead individuals increasing, while both numbers decreased on increasing υ.

(V) Our computation of the control reproduction number showed that $\mathcal{R}_c = 2.9562$. This suggests that the outbreak will continue in South Africa. However, this threshold quantity could be brought to a value less than unity ($\mathcal{R}_c = 0.9974$) if the aforementioned control measures are effectively implemented such that the effective contact rate β is reduced to $\beta_1 = 0.166$.

(VI) We computed the final size relations of the COVID-19 pandemic, and the associated attack rate, which beside being a measure for the severity of the pandemic suggests that the lower the attack rate is the sooner the peak time of the COVID-19 would arise.

(VII) Similar to [30,59], this study suggests that caution should be exercised before easing or lowering the COVID-19 alerts, so as to avoid to erase the gains made so far in curtailing the pandemic.

Our planned research project for the near future is to study the transmission dynamics of COVID-19 in the Western Cape Province. In the past few weeks and while finalizing this paper (mid June 2020), we have observed alarming trends in the estimated (cumulative total) numbers of COVID-19 confirmed cases and deaths in the Western Cape Province and its capital Cape Town (65% of the entire country) [35]. Western Cape has been declared the epicenter for COVID-19 in South Africa. However, this province has been exemplary in conducting the highest number of tests in the country (a total of 194939 tests *i.e.* 20%), and in identifying hotspot transmission areas or super-spread events. When designing the model for Western Cape, we need to take into account the framework of [36] in carefully sub-dividing the isolation compartment since hospitals, ICUs and other healthcare facility are already overwhelmed in the province (*viz.* 1425 COVID-19 cases are hospitalized including 230 in ICUs) .

Declaration of competing interest

The authors declare that they have no known competing financial interests or personal relationships that could have appeared to influence the work reported in this paper.

Acknowledgments

The authors acknowledge the support of the South African DST/NRF SARChI Chair in Mathematical Models and Methods in Bioengineering and Biosciences. The authors are grateful to the Handling Editor and the anonymous reviewers who have immensely contributed to improve the manuscript.

References

[1] World Health Organization, Situation Report - 166, 2020.
[2] Worldometer, 2020, (Worldometer-20) (Accessed July, 2020).
[3] Center for Systems Science and Engineering at Johns Hopkins University, COVID-19. Github Repository, 2020, (JohnsHopkins-20). (Accessed March/2020).
[4] B.L. Tesini, Coronaviruses and Acute Respiratory Syndromes (COVID-19, MERS and SARS), MSD Manuals on COVID-19, Merck and Co. Inc. Kenilworth, NJ, USA, 2020, (Tesini-20).
[5] World Health Organization, China's latest SARS outbreak has been contained, but biosafety concerns remain, Update 7, 2004. (WHO-SARS).
[6] M. Ceccarelli, M. Berretta, E.V. Rullo, G. Nunnari, B. Cacopardo, Differences and similarities between Severe Acute Respiratory Syndrome (SARS)-Coronavirus (CoV) and SARS-CoV-2. Would a rose by another name smell as sweet?, Eur. Rev. Med. Pharmacol. Sci. 24 (5) (2020) 2781–2783, (Ceccarelli).
[7] National Institute of Health. COVID-19, MERS AND SARS. (NIH-20).
[8] A.B. Gumel, S. Ruan, T. Day, J. Watmough, F. Brauer, P. van den Driessche, D. Gabrielson, C. Bowman, M.E. Alexander, S. Ardal, J. Wu, B.M. Sahai, Modelling strategies for controlling SARS outbreaks, Proc. R. Soc. Lond. B 271 (2004) 2223–2232.
[9] National Institute of Communicable Diseases, South Africa, Clinical management of suspected and confirmed COVID-19 diseases (Version 3), 2020, (NICD-20). (Accessed April 2020).
[10] S. Usaini, AS. Hassan, SM. Garba, JM-S. Lubuma, Modeling the transmission dynamics of the Middle East Respiratory Syndrome Coronavirus (MERS-CoV with latent immigrants, J. Interdiscipl. Math. 22 (6) (2019) 903–930.
[11] N.M. Ferguson, D. Laydon, G. Nedjati-Gilani, N. Imai, K. Ainslie, M. Baguelin, S. Bhatia, A. Boonyasiri, Z. Cucunub?a, G. Cuomo-Dannenburg, et al., Impact of Non-Pharmaceutical Interventions (NPIs) To Reduce COVID-19 Mortality and Healthcare Demand, Imperial College COVID-19 Response Team, London, 2020, (Ferguson-20).
[12] Joint Mission Report of the WHO-China Joint Mission on Coronavirus Disease 2019 (COVID-19), 2020, (JointMission-20). (Accessed April, 2020).
[13] S.E. Eikenberry, M.Muncuso, E. Iboi, T. Phan, E. Kostelich, Y. Kuang, A.B. Gumel, To mask or not to mask: Modeling the potential for face mask use by the general public to curtail the COVID-19 pandemic, Infect. Dis. Model. 5 (2020) 293–308, (Eikenberry-20).
[14] World Health Assembly, Global overview of an emerging novel coronavirus (MERS-CoV), 2013, (WorldHealthAssembly-20).
[15] D. Bernoulli, Essai d'une nouvelle analyse de la mortalité causée par la petite vérole et des avantages de l'inoculation pour la prévenir, Hist. Acad. R. Sci. Mém. Math. Phys. (1760) 1–45.
[16] W.O. Kermack, A.G. McKendrick, A contribution to the mathematical theory of epidemics, Proc. R. Soc. Lond. Ser. A Math. Phys. Eng. Sci. 115 (772) (1927) 700–721.
[17] G. Macdonald, The Epidemiology and Control of Malaria, Oxford University Press, London, New York, Toronto, 1957.
[18] R. Ross, The Prevention of Malaria, John Murray, London, 1911.
[19] G. Chowell, P.W. Fenimore, M.A. Castillo-Garsow, C. Castillo-Chavez. SARS outbreaks in Ontario, Hong Kong And Singapore: the role of diagnosis and isolation as a control mechanism, J. Theoret. Biol. 224 (1) (2003) 1–8.
[20] J. Lee, G. Chowell, E. Jung, A dynamic compartmental model for the middle east respiratory syndrome outbreak in the republic of Korea: A retrospective analysis on control interventions and superspreading events, J. Theoret. Biol. 408 (2016) 118–126.
[21] M. Lipsitch, T. Cohen, B. Cooper, J.M. Robins, S. Ma, L. James, G. Gopala, et al., Transmission dynamics andccontrol of severe acute respiratory syndrome, Science 300 (5627) (2003) 1966–1970, (Lipsitch).
[22] W. Wang, S. Ruan, Simulating the SARS outbreak in Beijing with limited data, J. Theoret. Biol. 227 (3) (2004) 369–379.
[23] Z. Zhao, F. Zhang, M. Xu, K. Huang, W. Zhong, W. Cai, et al., Description and clinical treatment of an early outbreak of severe acute respiratory syndrome in guangzhou, PR China, J. Med. Microbiol. 52 (8) (2003) 715–720, (Zhang-20).
[24] Z.-Q. Xia, J. Zhang, Y.-K. Xue, G.-Q. Sun, Z. Jin, Modeling the transmission of middle east respiratory syndrome corona virus in the Republic of Korea, PLoS One 10 (2015) e0144778.
[25] R. Anguelov, J. Banasiak, C. Bright, J. Lubuma, R. Ouifki, The big unknown: the asymptomatic spread of COVID-19, J. Biomath. 9 (1) (2020) (Anguelov-20).
[26] G.C. Calafiore, C. Novara, C. Possieri, A modified SIR model for the COVID-19 contagion in Italy, 2020, arXiv:2003.14391, (Calafiore-20) (Assessed May 2020).
[27] A.J. Kucharski, T.W. Russell, C. Diamond, Y. Liu, J. Edmunds, S. Funk, et al., Early dynamics of transmission and control of COVID-19: a mathematical modelling study, Lancet Infect. Dis. 5 (5) (2020) (Kucharski-20).
[28] K.O. Kwok, W.I. Wei, F. Lai, S.Y.S. Wong, J. Tang, Herd immunity-estimating level required to halt the COVID-19 epidemics in affected countries, J. Infect. 80 (2020) e32–e33, (Kwok-20).
[29] K. Mizumoto, G. Chowell, Transmission potential of the novel coronavirus (COVID-19) onboard the Diamond Princess Cruises Ship, 2020, Infect. Dis. Model. 5 (2020) 264–270, (Mizumoto-20).
[30] C.N. Ngonghala, E. Iboi, S. Eikenberry, M. Scotch, C.R. MacIntyre, M.H. Bonds, A.B. Gumel, Mathematical assessment of the impact of non-pharmaceutical interventions on curtailing the 2019 novel Coronavirus, Math. Biosci. 325 (2020) 108364, (Ngonghala-20). (Accessed 18 May 2020).
[31] J.T. Wu, K. Leung, G.M. Leung, Nowcasting and forecasting the potential domestic and international spread of the 2019-nCoV outbreak originating in Wuhan, China: a modelling study, Lancet 395 (10225) (2020) 689–697, (Wu-20).
[32] South Africa's policy response to the COVID-19 pandemic, Trade Law Centre-tralac News, 2020, (SAResponsetoCovid-19).
[33] World Health Organization, Laboratory testing strategy recommendations for COVID-19: interim guidance, 2020, (WHO-Lab).
[34] National Health Laboratory Service, Implementation of the preparedness and upscaling plan as of 7 april, 2020, 2020, (NHLS-20).
[35] Coronavirus South Africa (Wits in partnership with NRF, iThemba Labs and Data Convergence), COVID-19 South Africa Dashboard, (Covid19sa).
[36] South African COVID-19 Modelling Consortium (Prepared by MASHA, HE2RO, and SACEMA), Estimating cases for COVID-19 in South Africa, 2020, (ModellingConsortium-20) and (Update). (Accessed 6 May and 12 2020).
[37] South Africa Health Department, COVID-19 environmental health guidelines, 2020, (SAEnvironment-20).
[38] South Africa Health Department, Guidelines for quarantine and isolation in relations to COVID-19 exposure and infection, 2020, (SAQuarantine-Isolation-20).
[39] Y. Chen, L. Chen, Q. Deng, G. Zhang, K. Wu, L. Ni, Y. Yang, B. Liu, W. Wang, C. Wei, J. Yang, The presence of SARS-cov-2 RNA in the feces of COVID?19 patients, J. Med. Virol. (2020) (Y-Chen-20). (Accessed April 2020).
[40] L. Dietz, P.F. Horve, D.A. Coil, M. Fretz, J.A. Eisen, K. Van Den Wymelenberg, Novel Coronavirus (COVID-19) pandemic: built environment considerations to reduce transmission, Appl. Environ. Sci. (2019) (Dietz-20) (Accessed May 05, 2020).
[41] E. Goldman, Exaggerated risk of transmission of covid-19 by fomites, The Lancet 20 (2020) 892–893, (Godman-20).
[42] E. Ellis, Contaminated laundry piles up at Port Elizabeth Hospital, horrified officials, Maverick Citizen Eastern Cape, 2020, (Ellis-20).
[43] G. Medema, L. Heijnen, G. Elsinga, R. Italiaander, A. Brouwer, Presence of SARS-coronavirus-2 RNA in sewage and correlation with reported COVID-19 rrevalence in the early stage of the epidemic in The Netherlands, Environmental Science & Technology Letters (2020) (Medema-20). (Accessed May 2020).
[44] W. Randazzo, P. Truchado, E. Cuevas-Ferrando, P. Simón, A. Allende, G. Sánchez, SARS-CoV-2 RNA In wastewater anticipated COVID-19 occurrence in a low prevalence area, Water Res. 181 (2020) 115942, (Randazzo-20).
[45] A. Turton, Proof of Concept - Sewage Surveillance for Covid-19 in South Africa, 2020, (Turton-20) (Accessed 12 June 2020).

[46] B. Tang, X.Wang, Q. Li, N.L. Bragazzi, S. Tang, Y. Xiao, J. Wu, Estimation of the transmission risk of the 2019-nCoV and its implication for public health interventions, J. Clin. Med. 9 (462) (2020) (Tang-20) (Accessed April 2020).
[47] H. Zhao, Z. Feng, C. Castillo-Chavez, S.A. Levin, Staggered release policies for COVID-19 control: costs and benefits of sequentially relaxing restrictions by age, 2020, arXiv:2005-05.05549v1, (Zhao-20).
[48] H. Guo, M.Y. Li, Impacts of migration and immigration on disease transmission dynamics in heterogeneous populations, Discrete Continous Dyn. Syst. Ser. B 17 (7) (2012) 2413–2430.
[49] A. Gunia, Will COVID-19 ever go away? Time, 2020, (Gunia-20).
[50] C. Yang, J. Wang, A mathematical model for the novel coronavirus epidemic in Wuhan, China, Math. Biosci. Eng. 17 (3) (2020) 2708–2724, (Yang-20).
[51] B. Ivorra, M.R. Ferrández, Mathematical modeling of the spread of the coronavirus disease 2019 (COVID-19) taking into account the undetected infections: the case of China, Commun. Nonlinear Sci. Numer. Simul. (2020) 105303, (Ivorra-20) (Accessed 30 April 2020).
[52] R. Li, S. Pei, B. Chen, Y. Song, T. Zhang, W. Yang, J. Shaman, Substantial undocumented infection facilitates the rapid dissemination of novel coronavirus (SARS-CoV2), Science 368 (6490) (2020) 489–493, (Li-20).
[53] J. Seladi-Schulman, How long does the coronaviruse leave on different surfaces?, Healthline (2020) (Seladi-20). (Accessed 29 April 2020).
[54] P. van den Driessche, J. Watmough, Reproduction numbers and sub-threshold endemic equilibria for compartments models of disease transmission, Math. Biosci. 180 (2002) 29–48.
[55] Y. Liu, A.A. Gayle, A. Wilder-Smith, J. Rocklös, The reproductive number of COVID-19 is higher compared to SARS coronavirus, J. Travel Med. 27 (2) (2020) taaa021. (Liu-20) (Accessed April 2020).
[56] J.P. LaSalle, The Stability of Dynamical Systems, in: Regional Conference Series in Applied Mathematics, SIAM, Philadelphia, 1976.
[57] J. Arino, F. Brauer, P. van den Driessche, J. Watmough, J. Wu, A final size relation for epidemic models, Math. Biosci. Eng. 4 (2) (2007) 159–175.
[58] F. Brauer, C. Castillo-Chavez, Mathematical Models in Population Biology and Epidemiology, second ed., Springer, 2012.
[59] E. Iboi, O.O. Sharomi, C. Ngonghala, A.B. Gumel, Mathematical modeling and analysis of COVID-19 pandemic in Nigeria, Proc. Niger. Acad. Sci. (2020) submitted for publication.
[60] A. Rogers, The Asian countries that beat COVID-19 have to do it again, 2020, WIRED (Wired) (Accessed on April 13, 2020).